**Supplement material for**

Fast Cloud Parameter Retrievals of MIPAS/Envisat

by

R. Spang, K. Arndt, A. Dudhia, M. Höpfner, L. Hoffmann, J. Hurley, R. G. Grainger, S. Griessbach, C. Poulsen, J.J. Remedios, M. Riese, H. Sembhi, R. Siddans, A. Waterfall, and C. Zehner

in

Atmospheric Chemistry and Physics

## S1: Altitude Correction

The absolute values of the engineering tangent altitudes connected with the MIPAS level 1b data are known to have uncertainties up to several kilometres (Kiefer et al, 2007). The discrepancies typically vary by about 1.5 km within one orbit (in the case of ESA processor version ≥IPF/4.61 and <IPF/4.67), but are more or less constant for a single profile. Thus, any cloud top determination algorithm based only on the level 1b dataset is exposed to the same errors.

The absolute pointing information can be retrieved either in terms of pressure at the tangent point (Ridolfi et al., 2000) or geometrical tangent altitudes (von Clarmann et al, 2003). Both methods retrieve the relative pointing information in geometric coordinates.

The following procedure is implemented to correct the L1b altitude information.

(1) The pressure information is used from the ESA operational level 2 (L2) processing (Raspollini et al., 2006) together with the geopotential altitude from ECWMF reanalysis data, and the corresponding conversion to geometric altitudes to retrieve the pressure-based 'true' altitude. Geometric tangent altitudes for spectra with no pressure retrieval (e.g. due to cloud contamination and typically below a certain number of good quality L2 retrievals in the stratosphere) were computed by using the distance of the engineering tangent altitudes with respect to the lowest altitude level with retrieved pressure information.

(2) If no L2-profile is available the correction introduced by Kiefer et al. (2007) for the engineering altitudes is applied. A database of mean tangent altitude corrections is tabulated from temperature-altitude retrievals (von Clarmann et al., 2003) for the time period September 2002 to March 2003. These values are mean corrections over single days for various latitude bins and are interpolated with respect to latitude and time to the corresponding L1b location during the processing.

(3) If the observation time of the L1b profile is outside of the certain range of the Kiefer et al. correction, no altitude correction is applied and the original engineering altitudes are used.

When applying these corrections, the tangent altitude is assumed to be accurate in the order of 500 m for option 1 and ~200 m for option 2, whereas the remaining uncertainty of option 3 is in the order of +/- 1.5 km (von Clarmann et al. 2003). However, item (3) was applied only for a marginal amount of the MIPAS profiles

## S2: Improved NAT/Ice classification

Due to the different absorption and scattering characteristics with respect to the wavelength and the particle type, colour ratios and brightness temperature differences (BTD) are valuable tools for cloud type classification. The identification of NAT follows the analysis of Spang and Remedios (2003) and the refinements of Höpfner et al. (2006a). Two colour ratios, the operational $CI_A$ and the so-called NAT index (NI),

a colour ratio of the mean radiances of the 819-821 $cm^{-1}$ divided by the 788.2-795.25 $cm^{-1}$ microwindows, show a significant separation for NAT particles with radii of less than 3 μm in the scatter diagram of measurements (see e.g. Figure 3 in Spang and Remedios, 2003), in modelled spectra (Figure 9 in Höpfner et al., 2006a), and in the framework of this more detailed study with the CSDB. An example of all modelled NAT spectra of the CSDB between 15 and 24 km in comparison to STS and ice spectra is presented in Figure.

A simple NI threshold function ($NI_{thres}$) was fitted to the data. The function is valid over a broad altitude range (12-25km):

$$NI_{thres}(CI_A) = (0.1536 + 0.71531 \cdot CI_A - 0.03003 \cdot CI_A^2)^{-1}$$

The curve takes into account the fact that all modelled STS and ice spectra fall into the area below the threshold curve (not shown). The curve can be applied in the $CI_A$ range from 0.5 to 6, which covers optically thick to thin conditions. Spectra with $CI_A$ >6 are extreme events with low amount s of cloud in CSDB spectra and cannot be differentiated from cloud-free spectra. For classification purposes, it is necessary to compute $CI_A$ and $NI$ for the measured spectrum. Then the $FLAG_{NAT}$ is set to one if $NI > NI_{thres}$.

Similar to the $NI$ approach, the modelled spectra indicate that it is possible to differentiate between ice and STS with a BTD between 832.3-834.4 $cm^{-1}$ and 947.5-950.5 versus $CI_A$ similar to Figure S2.1 and presented in Figure S2.2a. A separation threshold function is now defined $ICESTS(CI_A)$ (dashed line). However, for ice versus NAT particles this differentiation method becomes inconclusive. NAT particle radii greater than 3 μm do overlap with the region where the ice particles appear (Firure S2.2b). A second threshold function $ICENAT(CI_A)$ is defined. Finally, a combination of these two constraints and the NAT index constraint allows an improved and distinct classification of ice spectra by:

$$BTD_{833\text{-}948} > ICENAT(CI_A) \quad \Rightarrow \quad FLAG_{ICE} = 1$$

$$ICENAT(CI_A) > BTD_{833\text{-}948} > ICESTS(CI_A) \quad \wedge \quad FLAG_{NAT} = 0 \quad \Rightarrow \quad FLAG_{ICE} = 1$$

A more generalised form of a multi-BTD approach is realised by the naive Bayes classification introduced in Appendix 3.

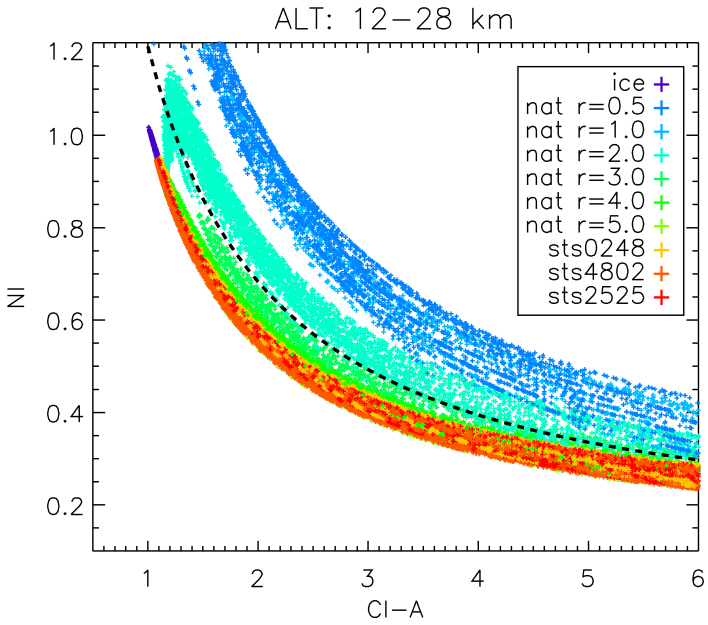


**Figure S2.1:** Correlation of cloud index $CI_A$ versus the colour ratio for NAT particle identification, the so-called NAT index (NI), in the latitude range 12-28 km. The radius dependency for NAT is colour-coded in green to light blue (0.5 to 5 µm). Dark blue crosses are related to ice and are mainly superimposed by STS symbols.

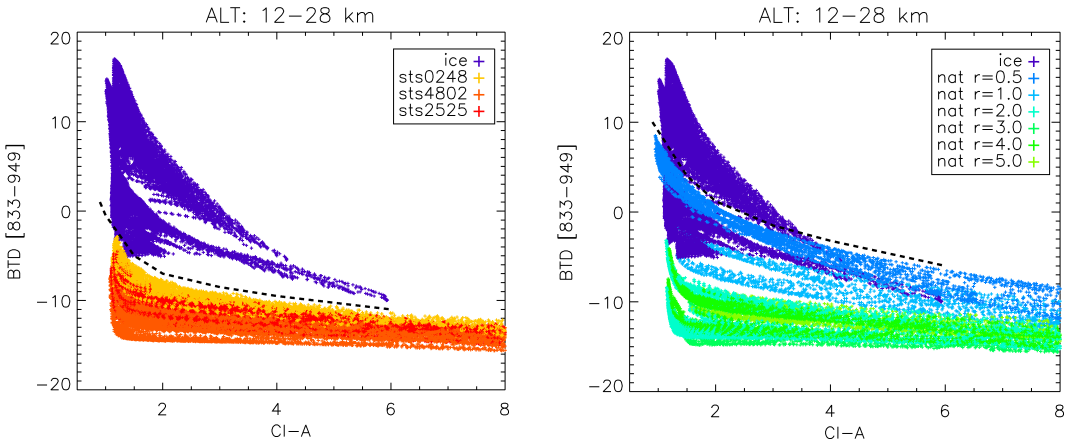


**Figure S2.2:** Threshold functions (dashed line) for ice/STS (left) and ice/NAT (right) differentiation based on CSDB spectra in the altitude range 12-28 km for $CI_A$ versus BTD of the mean radiances of 832.3 to 834.4 $cm^{-1}$ and 947.5 to 950.5 $cm^{-1}$. Dependency on STS composition (e.g. 0248 := 2% $HNO_3$ and 48% $H_2SO_4$ in orange to red) and radius (0.5 to 5 µm in green to light blue) are colour coded, respectively.

## S3: Cloud type classification with naive Bayes classifier

For a statistical classification of different cloud types a "naive Bayes classifier" was applied to CSDB spectra. This is a simple probabilistic classifier based on applying Bayes' theorem with strong (naive) independence assumptions. The classifier is trained by utilising the cloud radiance database prepared from the CSDB (Section 3.3) with one wavenumber resolution subset of spectra. Individual MIPAS measurements

are classified on the basis of multiple brightness temperature differences derived from the corresponding radiance data. In spite of the over-simplified assumptions, the naive Bayes classifier seems to work reasonably well for various applications.

**Naive Bayes classification**

For an overview of the method, we follow the description from Hanson et al., (1991). Naive Bayes classifiers can handle an arbitrary number of independent variables whether continuous or categorical. Given a set of variables, $X = \{x_1, x_2, \ldots, x_d\}$, the aim is to construct the probability for the event $C_j$ among a set of possible outcomes $C = \{c_1, c_2, \ldots, c_d\}$. Using Bayes' rule:

$$p(C_j \mid x_1, x_2, ..., x_d) = p(x_1, x_2, ..., x_d \mid C_j)\, p(C_j)$$

where $p(C_j \mid x_1, x_2, \ldots, x_d)$ is the posterior probability of class membership, i.e., the probability that $X$ belongs to $C_j$. Since naive Bayes assumes that the conditional probabilities of the independent variables are statistically independent we can perform a decomposition to a product of terms

$$p(X \mid C_j) = \prod_{k=1}^{d} p(x_k \mid C_j),$$

and rewrite the posterior as

$$p(C_j \mid X) = p(C_j) \prod_{k=1}^{d} p(x_k \mid C_j). \qquad \text{(A1)}$$

Using Bayes' rule above, we label a new case $X$ with a class level $C_j$ that achieves the highest posterior probability.

**Training the classifier**

All possible brightness temperatures are computed for all input classes of spectra that represent a certain cloud class of the CSDB. We tested various microwindow sizes between 0.5 and 1 $cm^{-1}$, whereby the most robust results were obtained for 1 $cm^{-1}$ and selected for the implementation. The results were subsumed under histograms for each class and BTD. For the histograms, various bin sizes were tested for BTD (1-4 K) and finally 4 K was selected. The next step was to identify the ratios with the highest information content for cloud classification. Therefore the CSDB spectra were analysed. The product probabilities for the brightness temperatures were computed according to Equation A1. The class assignment is related to the highest resulting probability. Since the cloud type (classification) of the modelled input spectra is well known, a score value of correctness can be evaluated which then allows the optimal ratios to be selected by maximizing the correctly assigned spectra.

**Implementation**

The histograms of the selected optimal ratios for each class discussed above provide the basis for the classification method. Large overlap in the histograms indicates more

difficulties in classification. Each brightness temperature difference of an input spectrum can be attributed to a specific probability $p_i$ in each class (cloud type). All selected brightness temperature differences then constitute a product probability

$$P_j = \prod_{i=1}^{N} p_{i,j}$$

for each potential cloud class ($j$: histogram class) over all selected MW pairs ($i$: number of histograms). A maximum of 10 MW pairs were selected. The maximum of $\boldsymbol{P}=\{P_1,\ldots,P_m\}$ explains the assignment to the cloud type class. As a consequence, it is possible to assign every single spectrum to a certain input cloud type.

For polar winter conditions above 12 km altitude, the processor is set up to distinguish ice, NAT and STS ($m$=3). Below this altitude and for other seasons and latitudes, the classification only distinguishes liquid and ice water clouds ($m$=2). Additional refinements improve the results of the Bayes classification. For example, selection of the optimised histograms for specific latitude bands and seasons as well as for a defined range of optical thicknesses of the clouds (where $CI_A$ can act as a good proxy for optically thickness) results in better training results of the method.

For application in the processor look-up tables of histograms for various latitude bands and $CI_A$ ranges are provided. Generally, in the data processing the classification, macro-, and micro- retrievals are restricted to the first 2-3 cloudy spectra in a MIPAS scan.

An extension of the CSDB with aerosol spectra is planned and would give the opportunity for a more detailed cloud particle differentiation in the troposphere, for example between background aerosol, volcanic ash, liquid, and ice water clouds.

## S4: References Supplement

Hanson, R., Stutz, J., and Cheeseman, P., Bayesian Classification Theory, NASA, Technical Report FIA-90-12-7-01, May, 1991.

Höpfner, M., Luo, B. P., Massoli, P., Cairo, F., Spang, R., Snels, M., Donfrancesco, G. D., Stiller, G., von Clarmann, T., Fischer, H., and Biermann, U.: Spectroscopic evidence for NAT, STS, and ice in MIPAS infrared limb emission measurements of polar stratospheric clouds, Atmos. Chem. Phys., 6, 1201–1219, doi:10.5194/acp-6-1201-2006, 2006a.

Spang, R., and Remedios, J., Observations of a distinctive infra-red spectral feature in the atmospheric spectra of polar stratospheric clouds measured by the CRISTA instrument, Geophys. Res. Lett., 30, 1875, 2003.